Supplementary Information, Appendices – "Uranium Particle Age Dating, Aggregation, and Model Age Best Estimators"

Evan E. Groopman[1], Todd L. Williamson[1], Timothy R. Pope[2], Michael G. Bronikowski[3], Spencer M. Scott[3], Matthew S. Wellons[3]

[1]Materials Measurement Science Division, National Institute of Standards and Technology, Gaithersburg, MD, 20899, USA
[2]Pacific Northwest National Laboratory, Richland, WA, 99354, USA
[3]Savannah River National Laboratory, Aiken, SC, 29808, USA

Bayesian Model

The Bayesian age dating model was built using the Python package PyMC[1]. Figure 1 shows a schematic graph view of the model with cartoon representations of the model prior and posterior distributions. Priors are represented by unshaded ovals, log-likelihood models by shaded ovals, and deterministic or intermediate calculation values by rectangles. The model has five required and two optional inputs for the priors, plus constants for the total measurement times of ^{230}Th and ^{234}U. Required priors are the Th/U RSF measured in standards, ^{234}U decay constant (λ) from the literature, average detector background rate (μ_{bkgd_230}) with uncertainty, observed ^{230}Th counts from the particle (total signal at m/z = 230), and observed ^{234}U counts from the particle. The abundance sensitivity correction is shown but is optional. It requires the relative abundance sensitivity (μ_{abn_230}) from ^{235}U and its uncertainty, and the ^{235}U/^{234}U ratio measured in the particle.

The priors for the RSF, λ, μ_{bkgd_230}, μ_{abn_230}, and ^{235}U/^{234}U are all informative with well-defined uncertainties and are set as Gaussian distributions, with some truncated to be greater than zero to remain physical. The priors for the counts of ^{230}Th (μ_{230Th}) and ^{234}U (μ_{234U}) are set to be minimally informative with centers aligned with the number of observed counts and the standard deviations set to be 10× the counting statistical uncertainties. These are set to be broad Gaussian distributions truncated at 0 to maintain physical realism and ensure smoothness at higher values.

The sum of $\mu_{230Th} + \mu_{bkgd\_230} + \mu_{abn\_230}$ is set as the parameter of a Poisson log-likelihood model sampled against the observed number of m/z = 230 observations. An independent Poisson process is fit to the observed ^{234}U counts. The model age is calculated deterministically in the Bayesian model from the posterior distributions for the parameters:

$$Model\ Age = \frac{(\mu_{230Th}/ct_{230Th})/(\mu_{234U}/ct_{234U})}{RSF_{Th/U} \cdot \lambda_{234}} \qquad (1)$$

where ct_{230Th} and ct_{234U} are the count times for each isotope.

For each model age we ran 10 MCMC chains of 2500 samples with a tuning/burn-in of 2000 samples and "advi+adapt_diag" or "jitter+adapt_diag" initialization of the No , which almost always resulted in no sampling divergences.

WM_{exp}

In order to more fully investigate the behavior of different averaging techniques when combining mid68 estimators, we constructed a larger simulation of 100 particles with the same $^{230}Th/^{234}U$ target ratio of $1{\times}10^{-5}$ and randomly chosen sizes as with the simulations in the main paper. All simulated particles had mid68 estimators calculated from their model age posterior distributions. The aggregated value of the simulated particles was $(9.88 \pm 0.42){\times}10^{-6}$ (1σ), which was within statistical uncertainty of the target value (Figure 2 left panel, black dashed line). The WM_{exp}, AVG, and WM values of the set were $(9.89 \pm 0.46){\times}10^{-6}$ (1 σ), $(10.08 \pm 0.43){\times}10^{-6}$ (1 σ), and $(8.36 \pm 0.54){\times}10^{-6}$ (1 σ), respectively. The WM_{exp} showed the best agreement with the aggregated value. We then ran bootstrapping simulations where we generated

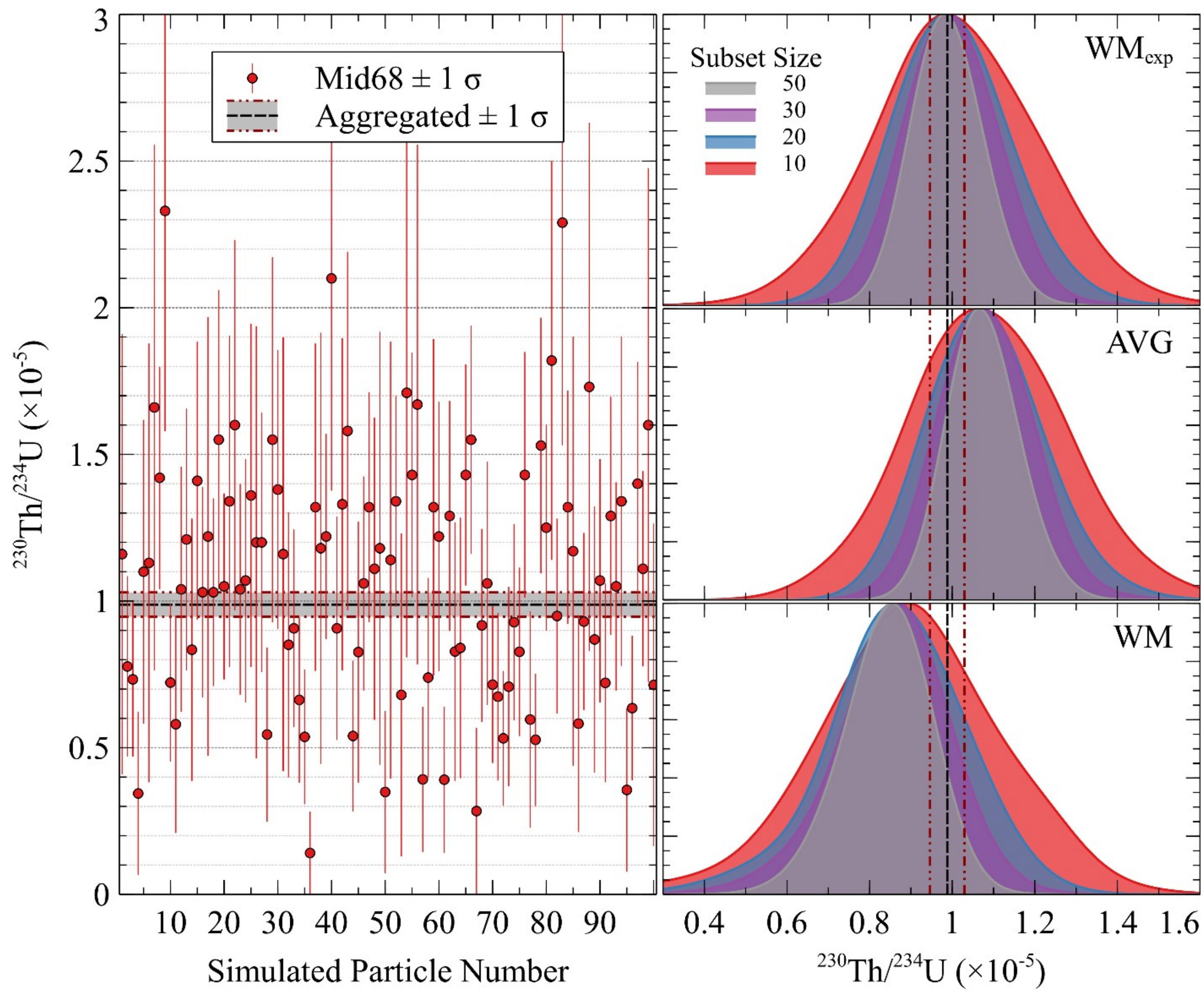

Figure 2: (Left) Simulation of large number of particles with $^{230}Th/^{234}U$ ratio of approximately $1{\times}10^{-5}$. (Right panels) aggregation of 200 random subsets each of different numbers of particles by several arithmetical averaging methods. The WM_{exp} method, which rescales the typical WM inverse-variance weights by raising them to the power of $(1/e)$, was the most accurate since the underlying particle model age distributions were usually asymmetric.

800 random subsamples from the dataset: 200 each with subsample sizes of 10, 20, 30, and 50 particles. From each of these subsamples we calculated each of the averages and generated kernel density estimates (KDE). Each KDE was generated from the 200 subsample averages, with a variable kernel bandwidth based on the SEM of each subsample[2]. The right panels of Figure 2 show the KDEs in comparison to the aggregated value. For larger subsample sizes, the KDEs were narrower, as expected. For all subsample sizes, WM_{exp} showed the best agreement with the aggregated value, whereas AVG was more likely to overestimate the $^{230}Th/^{234}U$ ratio and WM tended to underestimate it. This over- and under-estimation behavior of AVG and WM, respectively, was consistent for all sets of real and simulated data we tested. However, all of these averaging methods converge in scenarios where the ^{230}Th counts were larger and more approximately Gaussian.

As an additional example with real particle data, we reprocessed model ages of U005a particles from Szakal et al.[3] Figure 7. On the left panel of Figure 3 are the Bayesian mean ± SD estimators for the models ages and on the right are the mid68 ± width/2 estimators. The weighted and unweighted averages find better agreement with the aggregated value when using the mid68 estimators, as opposed to the mean ± SD. Among the averaging techniques for the mid68 points, WM_{exp} finds the best agreement with the aggregated value, particularly when the underlying posterior distributions are asymmetric, as in the example. As before, we experimented with harmonic and geometric mean algorithms, but these were not satisfactory.

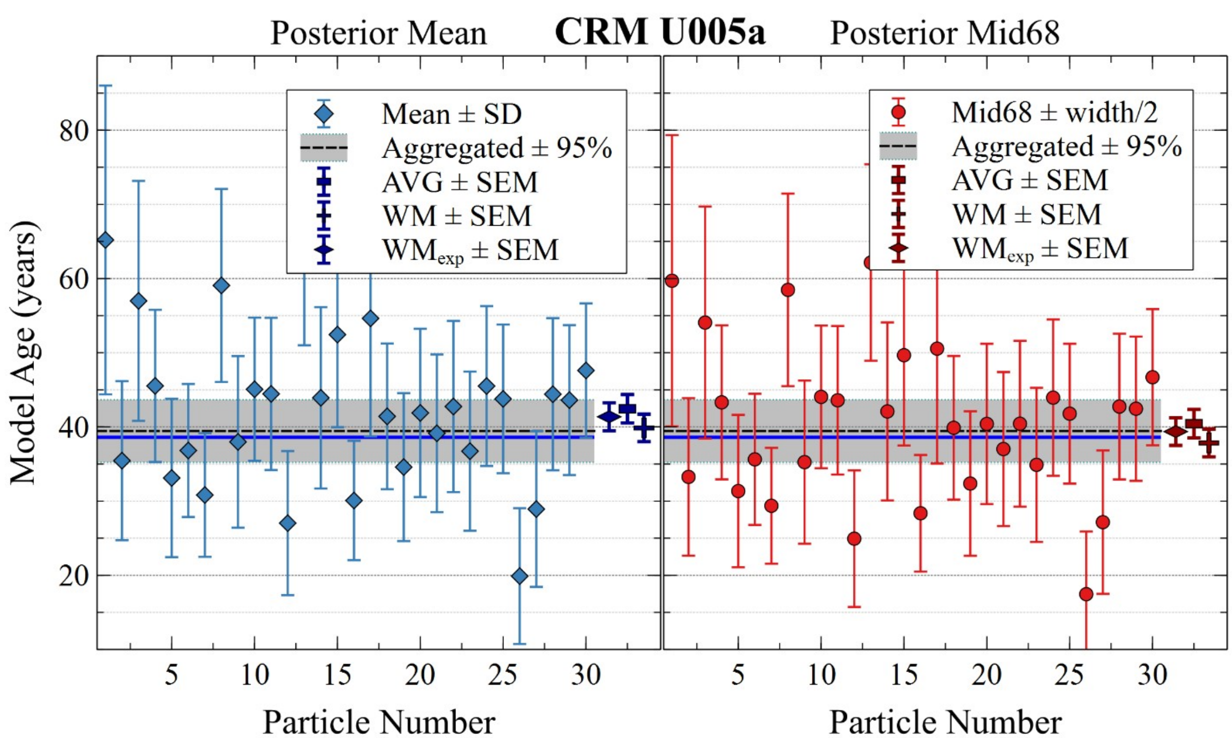

Figure 3: Comparison of aggregation methods using the Bayesian mean ± SD and mid68 ± half-width for CRM U005a particles measured by Szakal et al. (2019).

Coverage and Estimator Comparisons

Mid68 estimator uncertainty and coverage comparison plots for the Bayesian, Feldman-Cousins (FC), and Roe-Woodroofe (RW) methods. The Bayesian method achieves the closest to nominal coverage with the smallest relative and absolute uncertainties.

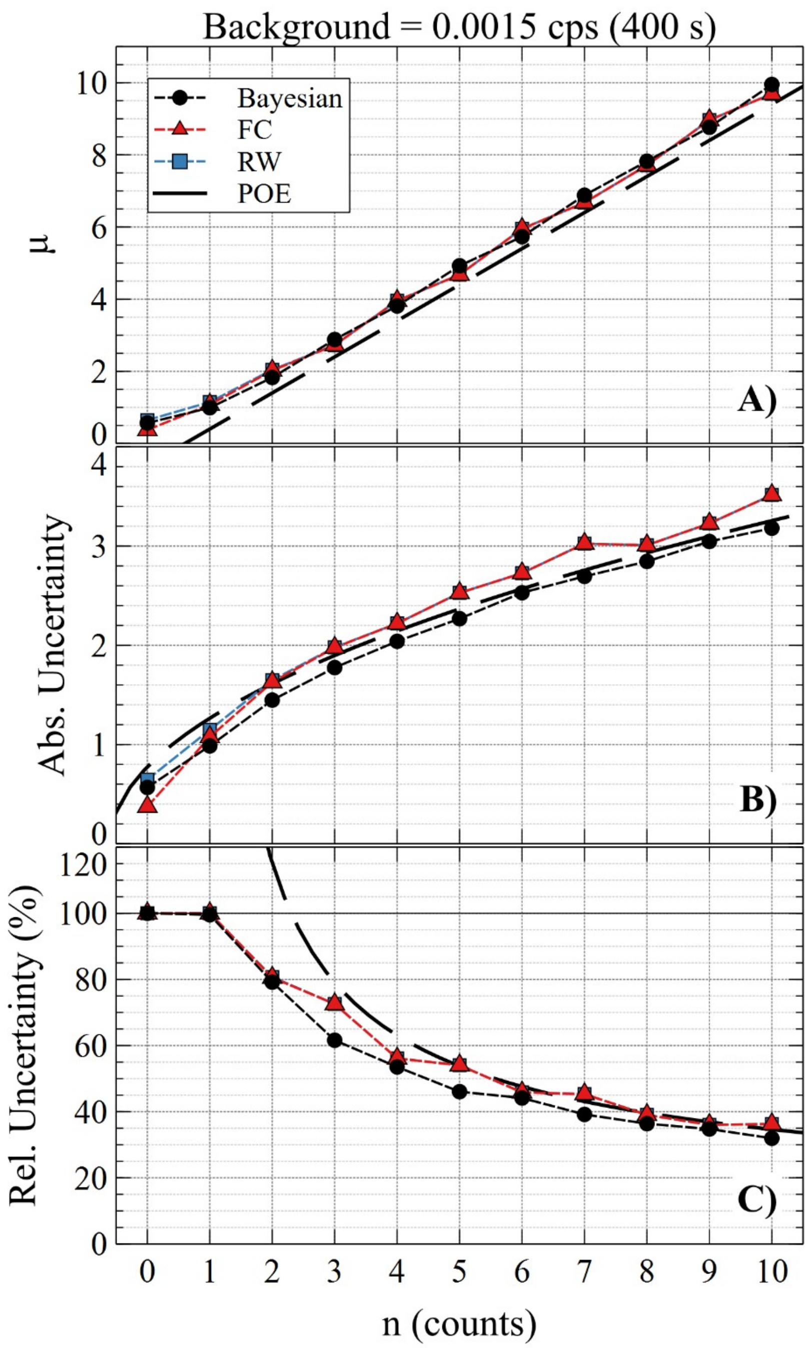

Figure 4: Location, absolute uncertainty, and relative uncertainty comparison of the mid68 estimator calculated using Bayesian, Feldman-Cousins (FC), and Roe-Woodroofe (RW) methods.

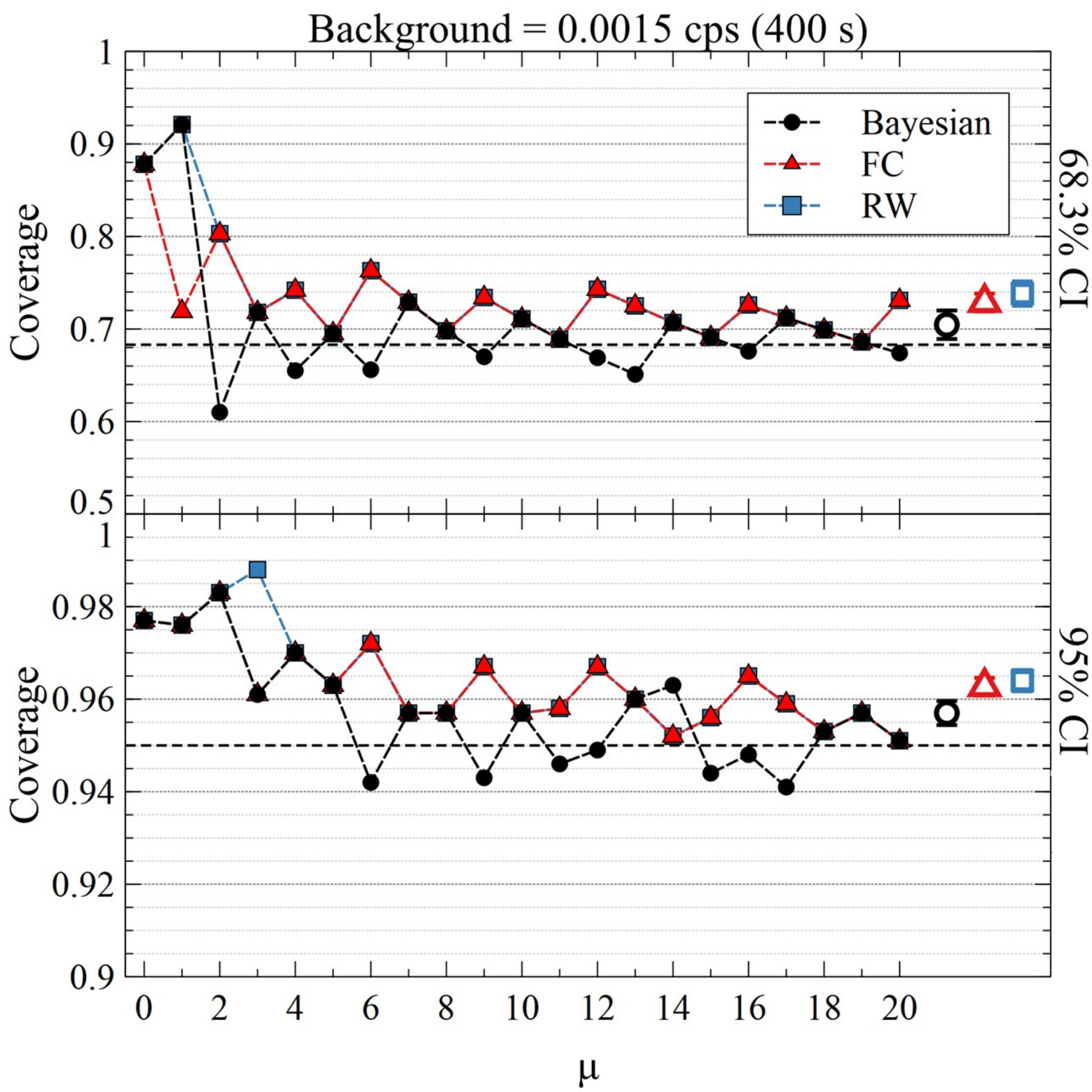

Figure 5: Comparison of 68.3 % and 95 % coverage for Bayesian, Feldman-Cousins (FC), and Roe-Woodroofe (RW) methods. Open symbols show the average coverage across the different Poisson parameter values.

Detector Background Comparisons

Additional figures are shown with comparisons of the impact of detector background on model age uncertainties for various U particle enrichments and masses.

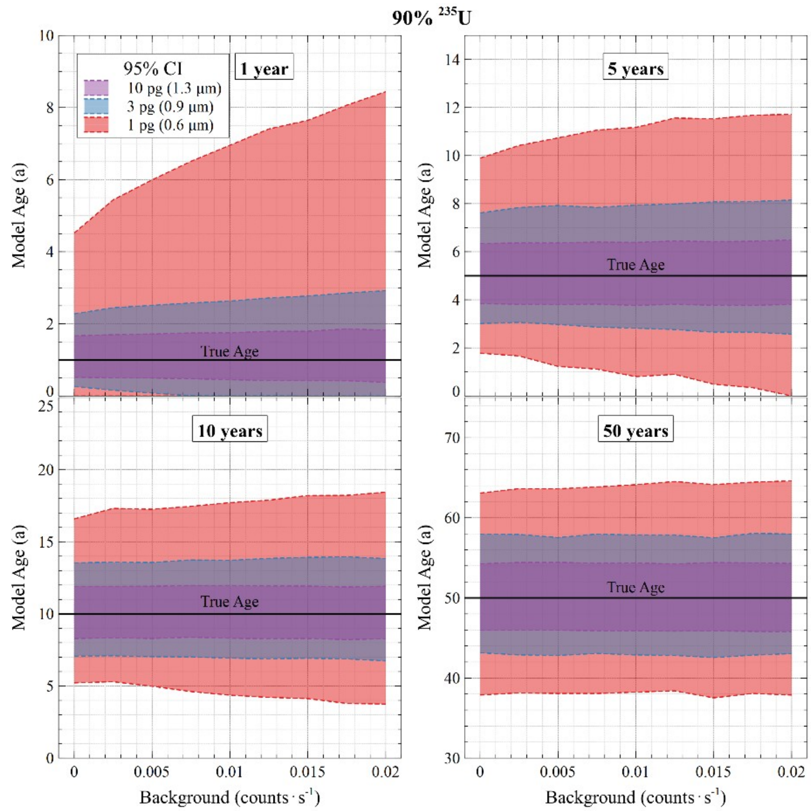

Figure 6: Effect of detector background rate on particles isotopically consistent with CRM U900 of difference masses and ages.

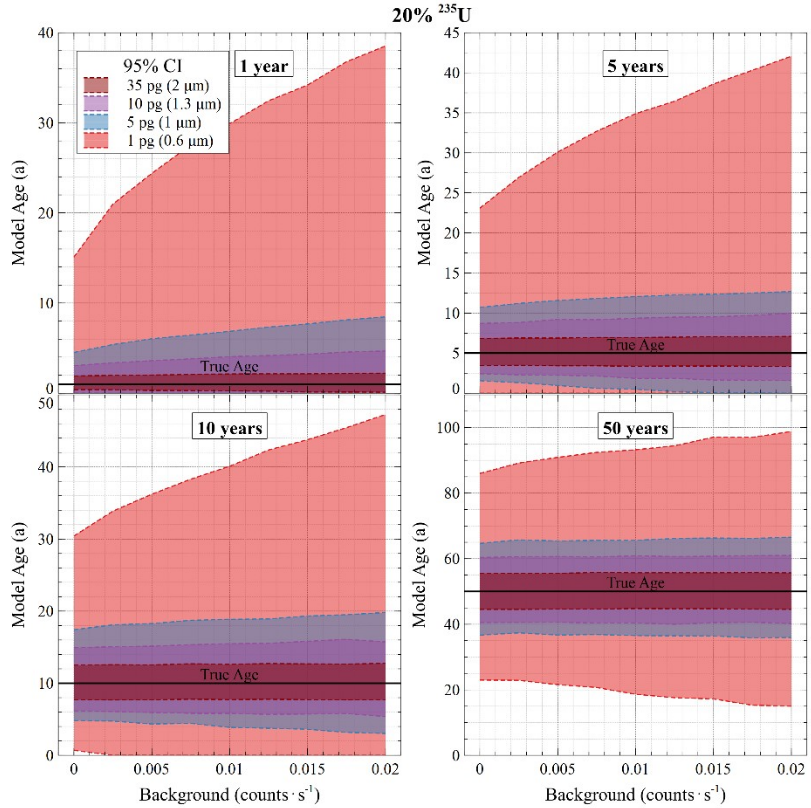

Figure 7: Effect of detector background rate on particles isotopically consistent with CRM U200 of difference masses and ages.

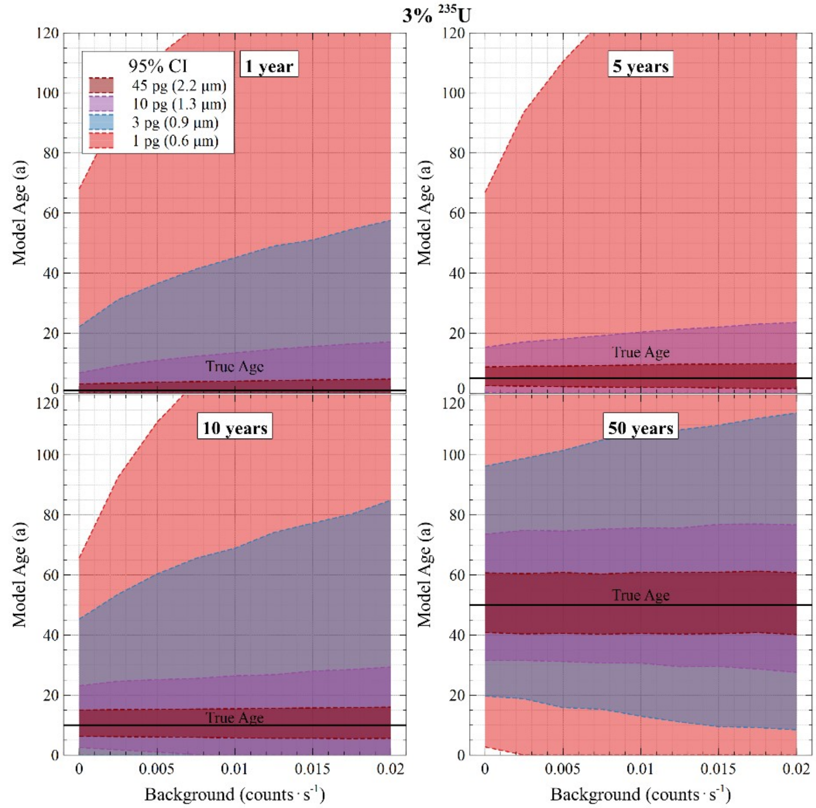

Figure 8: Effect of detector background rate on particles isotopically consistent with CRM U030A of difference masses and ages.

References:

1. O. Abril-Pla, V. Andreani, C. Carroll, L. Dong, C. J. Fonnesbeck, M. Kochurov, R. Kumar, J. Lao, C. C. Luhmann, O. A. Martin, M. Osthege, R. Vieira, T. Wiecki and R. Zinkov, *PeerJ Comput Sci*, 2023, **9**, e1516.
2. E. E. Groopman, L. R. Nittler, D. G. Willingham, A. P. Meshik and O. V. Pravdivtseva, *Applied Geochemistry*, 2021, **131**.
3. C. Szakal, D. S. Simons, J. D. Fassett and A. J. Fahey, *Analyst*, 2019, **144**, 4219-4232.